RSC Advances

PAPER

View Article Online
View Journal | View Issue

Cite this: *RSC Adv.*, 2021, **11**, 700

How to select ionic liquids as extracting agents systematically: a special case study for extractive denitrification processes†

Shurong Gao, *[abc] Jiaxin Jin,[ab] Masroor Abro,[c] Ruozhen Song,[c] Miao He[d] and Xiaochun Chen*[c]

Extractive denitrification (EDN) of shale oil using ionic liquids (ILs) as the extracting agent has good industrial prospects. In such processes, ILs with higher selectivity to N-compounds and lower solubility in shale oil are desired to improve the EDN efficiency, and reduce the loss of ILs and the contamination of shale oil. In the present study, we employed COSMO-RS to calculate the selectivity of 70 ILs to the typical N-compounds (pyridine, quinoline and indole). The influence of the IL structural characteristics, composition of shale oil and properties of N-compounds are investigated from a micro-level view with the σ-surface and σ-profile. The selectivity strongly depends on anionic species and it is greatly influenced by hydrogen bonding (HB) and $\pi-\pi$ interaction between N-compounds and ILs. ILs composed of $[H_2PO_4]^-$ and $[MeSO_3]^-$ with larger HB donor energy show higher selectivity to the basic N-compounds, while ILs composed of $[Ac]^-$ with larger π-electron cloud density show higher selectivity to the non-basic N-compounds. Anions with stronger polarity have lower solubility in shale oil. Moreover, experimental determinations of EDN indicated that $[C_4py][H_2PO_4]$/$[C_4mim][H_2PO_4]$ and $[C_2mim][Ac]$/$[C_2py][Ac]$ have good EDN performance for quinoline/pyridine with efficiency of 100% and for indole with efficiency of 91%, respectively. This work presents a theoretical basis to design and select ILs having higher selectivity for N-compounds and lower solubility in shale oil for use in denitrification.

Received 2nd November 2020
Accepted 14th December 2020

DOI: 10.1039/d0ra09316e

rsc.li/rsc-advances

1. Introduction

Shale oil, as an important alternative resource to petroleum, has attracted worldwide attention.[1] Considerable amounts of nitrogenous compounds (N-compounds), which may reduce the stability of shale oil in storage, increase the production of pollutants, and inhibit the processes of cracking and hydrotreating, is a key problem that prevents the development of shale oil.[2–4] Therefore, denitrification of shale oil is an important process in oil refining. The traditional hydrodenitrification (HDN)[5–7] is a widely employed technique in industry. Demanding harsh operating conditions, the ineffectiveness of HDN to remove heterocyclic N-compounds, and difficulty to meet the more stringent demands of N-content in fuel oil have driven researchers to explore alternative denitrification methods[8–10] to HDN.

Ionic liquids (ILs)[11–20] with desirable advantages (such as high steam pressure and nonvolatility, strong solubility of inorganic/organic compounds, easy recycling and so on) have attracted interest in extractive denitrification (EDN). Studies on EDN of conventional diesel or gasoline by ILs as extracting agent have been intensively studied, as shown in Table 1.[21–27] It can be observed that EDN employing ILs, which require mild operating conditions such as low pressure/temperature with no consumption of catalyst and hydrogen, can effectively remove N-compounds and have good denitrification effect. In our previous work,[25] we observed that almost 100% N-extraction efficiency for carbazole-containing fuel oil was obtained after a single extraction of <5 min contact time with $[BMI][N(CN)_2]$ and $[EMI][N(CN)_2]$ with 1 : 1 (w/w) IL : oil ratio under the ambient conditions. Therefore, EDN by ILs may offer a new method to denitrification of oil and present a good industrial prospect.

However, to our knowledge, EDN of shale oil by ILs has been rarely taken into account. N-removal efficiency is intensively studied,[21–27] while the systematic and comprehensive study about influence of ILs structural characteristics such as anionic nature on the denitrification performance is rarely reported.

[a]State Key Laboratory of Alternate Electrical Power System with Renewable Energy Sources, North China Electric Power University, Beijing, 102206, China. E-mail: gaoshurong@ncepu.edu.cn; Fax: +86-10-6443-3570; Tel: +86-10-6443-3570

[b]Research Center of Engineering Thermophysics, North China Electric Power University, Beijing, 102206, China

[c]Beijing Key Laboratory of Membrane Science and Technology, College of Chemical Engineering, Beijing University of Chemical Technology, Beijing 100029, PR China. E-mail: chenxc@mail.buct.edu.cn

[d]Office of Laboratory Safety Administration, Beijing University of Technology, Beijing 100124, China

† Electronic supplementary information (ESI) available. See DOI: 10.1039/d0ra09316e

Table 1 Research on the application of ILs in denitrification of fuel oil

ILs	Model oil	T/°C	IL : oil	N-extraction efficiency (%)	Extraction equilibrium	Ref.
[Bmim][BF_4]	Model oil	RT	1 : 1	60		21
[Bmim][$OcSO_4$]	Model oil	RT	1 : 1	41.2		21
[Emim][$EtSO_4$]	Model oil	RT	1 : 1	54.5		21
[Bmim]Cl	Carbazole	60	1 : 10	48	1 h	22
[OPy]Cl	Carbazole	60	1 : 10	58	1 h	22
[Bmim][BF_4]	Pyridine	RT	1 : 2	45	<0.5 h	22
[Bmim][BF_4]	Pyridine	RT	1 : 2	9	<0.5 h	23
[Bmim][BF_4]	Model oil	RT	1 : 1	1.5	15 min	24
[Bmin][$OcSO_4$]	Model oil	RT	1 : 1	0.7	15 min	24
[Emim][$EtSO_4$]	Model oil	RT	1 : 1	1.2	15 min	24
[Emim][DCA]	Pyridine	25	1 : 1	69.1		25
[$EtMe_2S$][DCA]	Pyridine	25	1 : 1	59.8		25
[S_2][DCA]	Pyridine	25	1 : 1	63.5		25
[Bmim][DCA]	Pyridine	25	1 : 1	72.7		25
[Bmim]Ac/$ZnAc_2$	Carbazole	40	1 : 1	100	1 min	26
[Bmim]Cl/$ZnAc_2$	Carbazole	40	1 : 1	94.5	30 min	26
[Bmim]Ac/$ZnAc_2$	Pyridine	40	1 : 1	36	1 min	26
[Bmim]Cl/$ZnAc_2$	Pyridine	40	1 : 1	95.1	30 min	26
[Bmim][$N(CN)_2$]	Carbazole	25	1 : 1	100	<5 min	25
[Emim][$N(CN)_2$]	Carbazole	25	1 : 1	100	<5 min	25
[S_2][$N(CN)_2$]	Carbazole	25	1 : 1	96	<5 min	25
[$EtMe_2S$][$N(CN)_2$]	Carbazole	25	1 : 1	83	<5 min	25
[Bmim][$N(CN)_2$]	Pyridine	25	1 : 1	72.7	5 min	25
[Emim][$N(CN)_2$]	Pyridine	25	1 : 1	69.1	5 min	25
[S_2][$N(CN)_2$]	Pyridine	25	1 : 1	63.5	5 min	25
[$EtMe_2S$][$N(CN)_2$]	Pyridine	25	1 : 1	59.8	5 min	25
[Bmim]Cl/$ZnCl_2$	Pyridine	25	1 : 1	>97	<5 min	27
[Bmim]Cl/2$ZnCl_2$	Pyridine	25	1 : 1	>97	<5 min	27
[Bmim][HSO_4]	Pyridine	25	1 : 1	>97	<5 min	27
[Hmim][HSO_4]	Pyridine	25	1 : 1	>97	<5 min	27
[Bmim]Cl/$ZnCl_2$	Carbazole	25	1 : 1	93.2	5 min	27
[Bmim]Cl/2$ZnCl_2$	Carbazole	25	1 : 1	90.1	5 min	27
[Bmim][HSO_4]	Carbazole	25	1 : 1	71.2	5 min	27
[Hmim][HSO_4]	Carbazole	25	1 : 1	24.2	5 min	27

Studies on EDN have shown that ILs have good denitrification effect which varies greatly due to their very different anionic and cationic structures.[25,27,28] Therefore, it is of great importance to choose appropriate ILs as extraction agents. The typical N-compounds such as pyridine, quinoline and indole are extracted into IL phase first and then removed through extraction in such new methods. Therefore, a suitable IL employed in denitrification technology should have higher selectivity to N-compounds and less solubility with shale oil, which are desired to improve the EDN efficiency, minimize the ILs loss and of shale oil contamination.

The performance of an extraction process greatly depends upon the suitable choice of solvent. Screening of ILs for extraction processes by experimental investigation is quite lengthy and uneconomical due to their availability in an enormous number, which can be overcome through the applications of thermodynamic models due to they are capable of predicting the activity coefficient, VLE and LLE data and so all.[29] Generally speaking, the most widely used models for VLE and LLE prediction in ILs include Wilson,[30] universal quasichemical (UNIQUAC),[31] non-random two-liquid (NRTL),[32] UNIFAC and modified UNIFAC models. The modified Flory–Huggins equation and a lattice model based on polymer solution models are also adopted to well-describe the phase diagrams.[33] The group contribution methods like UNIFAC and its modified variants are also employed to correlate the thermodynamic properties and LLE in ILs.[18] However, the key disadvantage of aforesaid models is their limited applications specifically for ILs due to lack of required parameters for most of ILs.[34]

On the other hand, the Continuum Solvation Model known as conductor-like screening model for real solvents (COSMO-RS) is an efficient predictive tool for thermodynamics properties and phase behaviors of ILs based systems such as enthalpies of vaporization,[35] gas solubility,[36] liquid–liquid equilibrium LLE[37,38] and capacity of ILs for hydrocarbons.[39] It is a well-established thermodynamic model requiring only the information on the atoms of the compounds without needing any experimental data, which can be extrapolated over new systems to achieve qualitative accuracy.[40] There has been a gradual evolution in variants of COSMO-RS *i.e.*, COSMO-SAC[41] and COSMO-RS (OI).[42] Over the last two decades, an adequate number of studies have used COSMO based models with purpose of LLE and thermodynamic parameters prediction to screen of ILs.[32,37,43] Banerjee *et al.*[44] used a modified variant of

COSMO-RS known as COSMO_LL to predict the LLE data of a number of ILs based ternary systems and obtained improved predictions for ternary systems. Gutiérrez *et al.*[45] performed the preselection of ILs for extractive distillation process employing COSMOtherm software by investigating the effect of anion and cation on the selectivity and activity coefficient. Zhou *et al.*[46] used COSMO-SAC model to screen ILs for separation of thioglycolic acid and water. They investigated the effect of anion and length of cation alkyl chain on selectivity and capacity. A few studies have been reported on employing COSMO-RS to predict the capacities of ILs for TS and DBT, *e.g.*, Kumar *et al.*[47] studied the capacity of 264 ILs for TS. Anantharaj *et al.*[48] reported the capacity of 168 ILs for TS and DBT and Song *et al.*[49] reported the capacity of 216 ILs for TS. These studies reveal that COSMO-RS and its variant models have great potential to screen suitable ILs for several separation applications.[50]

Compared with a very huge pool of ILs (about 10^{18} potential ILs exist), a very limited number of ILs was studied experimentally in denitrification shown in Table 1. The aforementioned theoretical methods can desirably be employed to calculate selectivity of ILs to N-compounds. To our knowledge, determination of selectivity of ILs to N-compounds employing COSMO-RS is still a remainder.

In this work, a new coupled COSMO-RS based theoretical study and the experimental denitrification research is designed and achieved as shown in Fig. 1. (1) The selectivity of 70 kinds of ILs from the combination of 5 anions and 14 cations, (the short and full names with their chemical structures are summarized in Tables S1 and S2†) to pyridine, quinoline and indole (chemical structures are provided in Fig. 2) is computed using COSMO-RS; then the influence of ILs structural characteristics, composition of shale oil, properties of N-compounds are investigated from micro-level view with σ-surface and σ-profile. (2) Based on the selectivity of ILs to N-compounds, we selected several suitable ILs and studied their solubility with shale oil. (3) Finally, the selected ILs, which exhibit higher selectivity for N-components and smaller solubility with shale oil, are investigated by experiments of EDN. It should be noted that five kinds of anions, *i.e.*, $[Cl]^-$, $[Ac]^-$, $[Br]^-$, $[MeSO_3]^-$, and $[H_2PO_4]^-$,

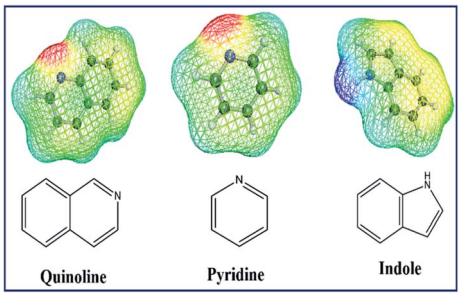

Fig. 2 σ-Surface and structure of quinoline, pyridine and indole.

are selected in this study because the anions are common and representative species which represent five types of ionic liquids, *i.e.*, chloride, acetate, bromide, sulfonate, phosphate based ILs, respectively. In the other side, pyrrolidinium, pyridinium and imidazolium are three kinds of the common cation family which are studied widely; therefore, we selected $[C_npyr]^+$, $[C_npy]^+$ and $[C_nmim]^+$ based ILs as the representative cations to perform the following study by COSMO-RS. In order to further investigate the influence of cation alkyl chain length, we also choose different alkyl chain on the base of each kind of cation family. For example, for the $[C_nmim]^+$ based ILs, we select $[C_1mim]^+$, $[C_2mim]^+$, $[C_3mim]^+$ and $[C_4mim]^+$.

2. Method

2.1 COSMO-RS

2.1.1. COSMO-RS calculations. The selectivity of IL for N-compounds and the solubility of ILs with shale oil are calculated by COSMO-RS[51–56] in this work. For the specific procedures of obtaining the anions and cations of different ILs and the molecular structure of typical N-compounds and the detailed description of COSMO-RS equations, we have elaborated on this in ESI.† Herein, the main equations used in this work are emphasized only.

The selectivity of IL for N-compounds is calculated by eqn (1),

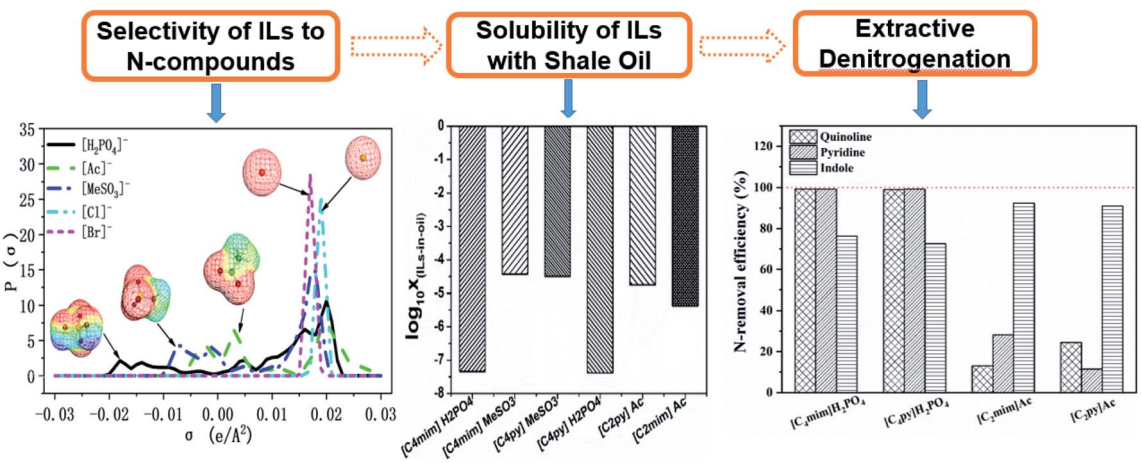

Fig. 1 Schematic diagram in this manuscript.

$$S_{12,\max} = S_{12}^{\infty} = \frac{\gamma_2^{\infty}}{\gamma_1^{\infty}} \quad (1)$$

where, γ_1^{∞} is the activity coefficient of component; N-compounds (pyridine, quinoline and indole) at infinite dilution in ILs; γ_2^{∞} is the activity coefficient of component; N-compounds at infinite dilution in shale oil.

The solubility of IL in shale oil is calculated by eqn (2),

$$\log_{10}(\chi_{IL}^{sol}) = [\mu_{IL}^{(P)} - \mu_{IL}^{(oil)} - \max(0,\Delta G_{fus})]/(RT\ln(10)) \quad (2)$$

where $\mu_{IL}^{(oil)}$ and $\mu_{IL}^{(p)}$ denote the chemical potential of the IL in shale oil and pure solute, respectively; ΔG_{fus} stands for Gibbs free energy of fusion.

2.1.2. σ theory. The theory of σ-profile is given in our published articles,[11,12] herein, we just emphasize on the theory of σ-surface used in this manuscript. σ-Surface indicates the shielding charge density of the molecular surface in the form of 3D structure through different colors, which can be used to analyze the polarity, hydrogen-bonding (HB) energies and π electron cloud of molecules. For example, the red part represents the negative surface shielding charge generated by the positive charge inside the molecule, the blue part represents the positive surface shielding charge region, the green part represents the neutral surface shielding charge region which means the molecules are non-polar, and the yellow part represents the π electron cloud density according to Klamt *et al.*[57] The σ-surface diagram of pyridine, quinoline and indole is shown in Fig. 2. For the basic N-compounds, *i.e.*, quinoline and pyridine, the negative shielding charge density near the nitrogen atom is large and it is red. Therefore, quinoline and pyridine can be used as HB receptors and they have high HB receptor energy. In contrast, indole, as a non-basic N-compound, has a high positive shielding charge density and it is blue, which means that indole can be used as HB donor and it has high HB donor energy. It also can be seen from Fig. 2 that the molecules of pyridine, quinoline and indole contain the π electron cloud density, which correspond to the yellow part in the diagram. However, the yellow area of indole molecule is the largest, that is, the π electron cloud density of indole is the largest. In a summary, pyridine and quinoline can be used as HB receptors, which are easy to be combined with HB donors; while indole can be used as a HB donor, which is easy to be combined with HB receptors.

2.2 Experiments

2.2.1. Chemicals. The information of chemicals used in this work is as follows: bromine ethane (>99.0%), bromobutane (>99.0%), Aladdin Reagent Co. Ltd; *N*-methylimidazole (>99.0%), Shanghai SenHao Fine Chemical; ethyl acetate (≥99.5%), acetone (≥99.5%), dichloromethane (≥99.5%), acetic acid (≥99.5%), *n*-octane (≥99.0%), cyclohexane (AR), *n*-octene (≥98.0%), cyclohexene (≥99.0%), toluene (≥99.5%), Beijing Chemical Works; nitrogen (≥99.9%), Beijing Yanan Gas Plant; quinoline (AR), pyridine (≥99.5%), indole (≥99.0%), Tianjin Fuchen Chemical.

2.2.2. Synthesis of ILs and shale oil

Synthesis of ILs. The synthesis method of $[C_4py][H_2PO_4]$, $[C_4mim][H_2PO_4]$, $[C_2mim][Ac]$ and $[C_2py][Ac]$ is as follows and the FT-IR spectrum of ILs is shown in Fig. S1–S4.† (1) $[C_4py][H_2PO_4]$: 0.5 mol pyridine was poured into a 100 ml round-bottom flask, then 0.55 mol bromobutane was poured slowly drop by drop through a constant pressure titration funnel and stirred vigorously at 70 °C for 24 h in inert atmosphere. The obtained liquid was washed using ethyl acetate for three times, later, through rotary evaporation, it was removed under vacuum at 60 °C for 60 min to get $[C_4py]Br$ as white solid. 0.1 mol $[C_4py]Br$ and 0.1 mol H_2PO_4 were put into a 100 ml round-bottom flask, then dichloromethane was used as the solvent and stirred vigorously at 25 °C for 9 h in inert atmosphere to get $[C_4py][H_2PO_4]$ as yellow oily viscous liquid. (2) $[C_4mim][H_2PO_4]$: 0.5 mol 1-methylimidazole was added into a 100 ml round-bottom flask, then 0.55 mol bromobutane was poured slowly drop by drop through a constant pressure titration funnel and vigorously stirred at 70 °C for 24 h under an inert atmosphere. The obtained liquid was washed using ethyl acetate for three times, similarly, the rotary evaporation was conducted to remove it under vacuum at 60 °C for 60 min to get $[C_4mim]Br$ as white solid. 0.1 mol $[C_4mim]Br$ and 0.1 mol H_2PO_4 were put into a 100 ml round-bottom flask, then dichloromethane was used as the solvent and stirred vigorously at 25 °C for 9 h under an inert atmosphere to get $[C_4mim][H_2PO_4]$ as yellow oily viscous liquid. (3) $[C_2mim][Ac]$: 0.5 mol 1-methylimidazole was added into a 100 ml round-bottom flask, then 0.55 mol bromine ethane was poured slowly drop by drop through a constant pressure titration funnel and stirred vigorously at 30 °C for 9 h in inert atmosphere. The obtained liquid was washed using ethyl acetate for three times, similarly, the rotary evaporation was conducted to remove it under vacuum at 60 °C for 60 min to get $[C_2mim][Br]$. 0.1 mol $[C_2mim][Br]$ and 0.1 mol acetic acid were put into a 100 ml round-bottom flask, then acetone was used as the solvent and stirred vigorously at 25 °C for 24 h in inert atmosphere to get $[C_2mim][Ac]$ as colorless transparent oily liquid. (4) $[C_2py][Ac]$: 0.5 mol pyridine was added into a 100 ml round-bottom flask, then 0.55 mol bromine ethane was poured slowly drop by drop through a constant pressure titration funnel and stirred vigorously at 30 °C for 9 h in inert atmosphere. The obtained liquid was washed using ethyl acetate for three times, which was removed by rotary evaporation under vacuum at 60 °C for 50 min to get $[C_2py][Br]$. 0.1 mol $[C_2py][Br]$ and 0.1 mol acetic acid were put into a 100 ml round-bottom flask, then acetone was used as the solvent and stirred vigorously at 25 °C for 24 h in inert atmosphere to get $[C_2py][Br]$ as dark yellow oily liquid.

Model shale oil preparation. Model shale oil with N-content of 2000 ppm, contained a mixture of *n*-octane, cyclohexane, *n*-octene, cyclohexene, toluene with the mass ratio of 3 : 1 : 2 : 1.5 : 2.5. Quinoline and pyridine as representative basic N-compounds and indole as representative non-basic N-compound (structures are given in Fig. 2) were investigated in the EDN.

2.2.3. Extractive denitrification and analysis

General procedure. In a typical EDN experiment, ILs and shale oil were poured into round-bottom flask where, these underwent reaction by stirring with a magnetic stirrer under certain temperature for a given time. The mixture was settled for 30 min to achieve phase-segregation and the oil (upper phase) was investigated.

Analysis of N-content in shale oil. The N-content of quinoline, pyridine and indole were analyzed by GC-112A gas chromatograph equipped with SGE-AC 20 60 m × 0.32 mm × 0.5 μm column. The gas chromatography (99.999% N_2) was pressurized at 50 °C and increased to 250 °C, the temperature at inlet was set to 250 °C, the injection volume was 0.2 μL and split ratio was 20 : 1. EDN efficiency E (%) and distribution coefficients K_N were calculated by eqn (3) and (4)

$$E\ (\%) = \frac{C_i - C_f}{C_i} \times 100 \quad (3)$$

$$K_N = \frac{(C_i - C_f)/m_{IL}}{C_f/m_{oil}} \quad (4)$$

where C_i and C_f are initial and final N-content and m_{IL} and m_{oil} are mass of ILs and shale oil, respectively.

3. Results and discussion

3.1 Validation of COSMO-RS prediction

Presently, we compared the COSMO-RS predicted liquid–liquid equilibrium data of the $[C_2mim]MeSO_3$ + pyridine/indole + *n*-hexadecane based system against the previously reported experimental data.[32] Fig. 3 shows a good agreement between COSMO-RS prediction of liquid–liquid equilibrium results and those obtained experimentally. The root-mean-square error for the system of $[C_2mim]MeSO_3$ + pyridine/indole + *n*-hexadecane between experimental results and COSMO-RS calculations is 2.06%/4.41%, respectively. Some studies also have proved the reliability of COSMO-RS for prediction of LLE data of IL-based systems qualitatively, also acceptable quantitatively in many cases.[11,12,51,56] Therefore, COSMO-RS is an effective tool to be employed in qualitative screening of ILs with regard to their liquid–liquid equilibrium data, components of shale oil and N-compounds.

It should be mentioned that (1) the selectivity is only valid for small concentrations of the N-compounds, *i.e.* the molecular solutes in their infinitely diluted solution with ILs. (2) In the COSMO-RS calculation, ILs are treated as electro-neutral mixtures of separated cations and anions, leading to the simulation is qualitatively accurate in some cases. (3) We only pay attention to the changing trend of the selectivity and the solubility values in order to find some regulars and provide the theoretical basis for designing and selecting of ILs used in the denitrification process of shale oil used in the follow-up experimental study.

3.2 Selectivity of ILs for N-component

The selectivity of ILs for N-components has great importance in EDN process. The higher the selectivity of ILs to N-compounds, the higher the N-removal efficiency can be obtained. In this study, toluene and octane, which represent aliphatic and aromatic hydrocarbons in shale oil respectively, were selected to investigate the selectivity of ILs to N-compounds. The selectivity of 70 kinds of ILs (from the combination of 5 anions and 14 cations) to pyridine, quinoline and indole was computed by COSMO-RS as presented in Fig. 4, 8 and 9, respectively.

3.2.1. Selectivity of ILs for pyridine. According to Fig. 4, comparing to cations, anions are more influential towards the selectivity of ILs to pyridine, because of their stronger polarity and hydrogen bonding than those of cations as shown in Fig. 5. For the same cation, the selectivity of ILs to quinoline in toluene/octane roughly increased as $[Cl]^- < [Ac]^- < [Br]^- < [MeSO_3]^- < [H_2PO_4]^-$. The influence of anions is explained with the help of σ theory[23,27] in Fig. 5. The peaks of $[Cl]^-$, $[Ac]^-$, $[Br]^-$, $[MeSO_3]^-$ and $[H_2PO_4]^-$ existing in the polar region of $\sigma > +0.0082$ e Å^{-2}, correspond to the red part in the σ-surface diagram and they can be used as HB receptors. While for $[MeSO_3]^-$ and $[H_2PO_4]^-$, several peaks are existed in the polar region of $\sigma < -0.0082$ e Å^{-2}, which correspond to the blue part

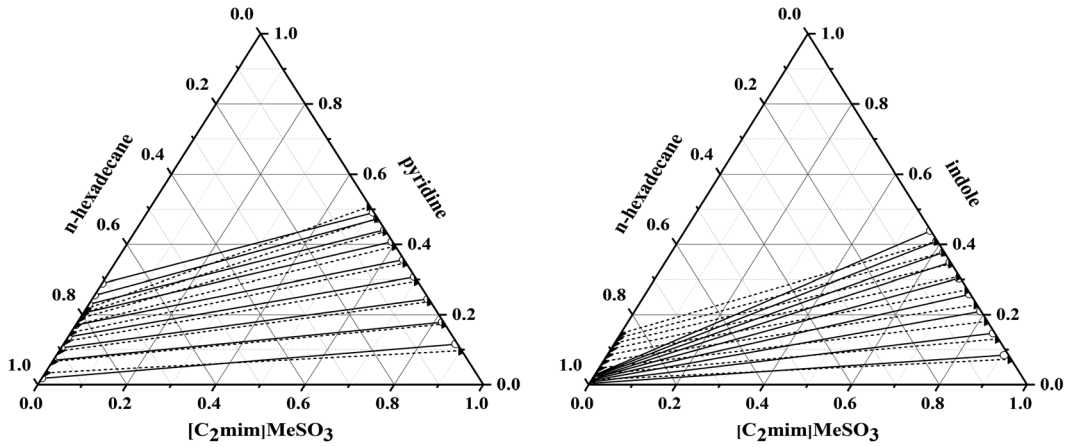

Fig. 3 Tie-lines for the ternary systems $[C_2mim]MeSO_3$ + pyridine/indole + *n*-hexadecane at 25 °C (empty circle and solid lines indicate experimental tie-lines, full triangle and dashed lines indicate COSMO-RS calculated tie-lines).

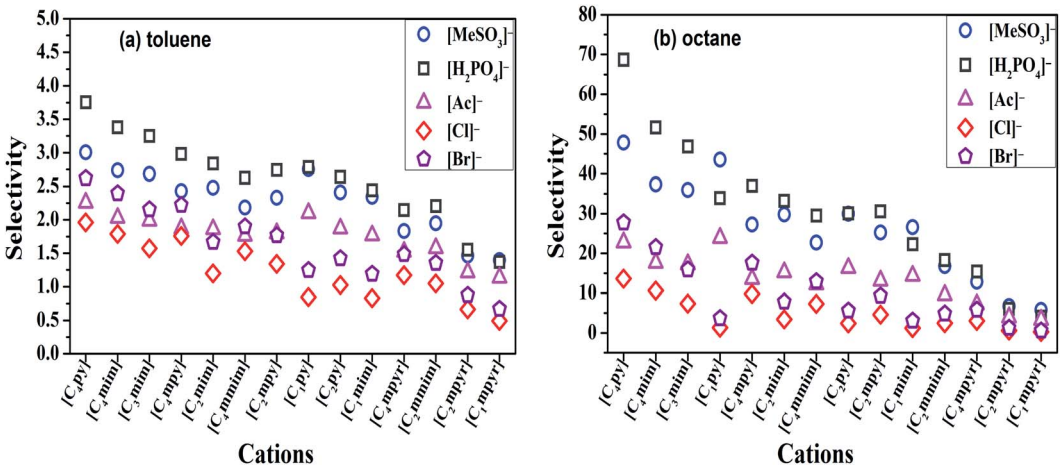

Fig. 4 Selectivity of ILs for pyridine in (a) toluene and (b) octane.

in the σ-surface diagram and they can also be used as HB donors. As a result, $[MeSO_3]^-$ and $[H_2PO_4]^-$ (as HB donors), which have hydrogen bonding with pyridine (as HB receptor) as seen in Fig. 6, result in higher selectivity of $[MeSO_3]^-$ and $[H_2PO_4]^-$ based ILs to pyridine.

In addition, the selectivity is also significantly affected by the composition of shale oil. As shown in Fig. 4, the selectivity of ILs to pyridine in octane (0.24–68.65) is larger than that in toluene (0.49–3.75). This is consistent with the experimental results of Anugwom *et al.*,[58] which indicated that for the model oil composed of aromatic hydrocarbon, ILs exhibited poor selective removal effect on pyridine. This might be related to the π–π interaction between π-electron on pyridine molecule (as seen in the yellow part of the σ-surface diagram in Fig. 6) and aromatic toluene ring. The σ profile results in Fig. 7 show that toluene is more polar than octane, where the main peaks of the σ profile of toluene are located in the polar region while those of octane are existed in the non-polar region. Based on the rule of "like dissolves like", polar N-compounds are more soluble in the more polar toluene. Therefore, ILs have higher selectivity to pyridine in the shale oil containing the less polar compounds such as octane.

3.2.2. Selectivity of ILs for quinoline. As shown in Fig. 8, the anionic nature and composition in shale oil also exhibited considerable effect on the selectivity of ILs to quinoline. $[MeSO_3]^-$ and $[H_2PO_4]^-$ (with higher HB donor energy) have strong hydrogen bonding with quinoline (with lager HB receptor energy), resulting in higher selectivity of the ILs composed of $[MeSO_3]^-$ and $[H_2PO_4]^-$ to quinoline. The selectivity of ILs to quinoline in octane (5.25–45.16) is higher than that in toluene (2.50–3.75).

In summary, ILs composed of anions as $[H_2PO_4]^-$ and $[MeSO_3]^-$, show higher selectivity to quinoline and pyridine in weaker polar compounds such as octane in shale oil. From Fig. 4 and 8, $[C_4py][H_2PO_4]$, $[C_4mim][H_2PO_4]$, $[C_4py][MeSO_3]$ and $[C_4mim][MeSO_3]$ are selected to remove the basic N-compounds in shale oil.

3.2.3. Selectivity of ILs for indole. Fig. 9 shows different ILs have different selectivity to the non-basic N-compounds, *i.e.*, indole, and the selectivity is ranged from 109.41 to 5379.38. Obviously, the selectivity of ILs to indole is much higher than that to pyridine and quinoline. It can be seen from Fig. 5 that the peaks of $[Cl]^-$, $[Ac]^-$, $[Br]^-$, $[MeSO_3]^-$ and $[H_2PO_4]^-$ are located in the polar region of σ > +0.0082 e Å^{-2}, which

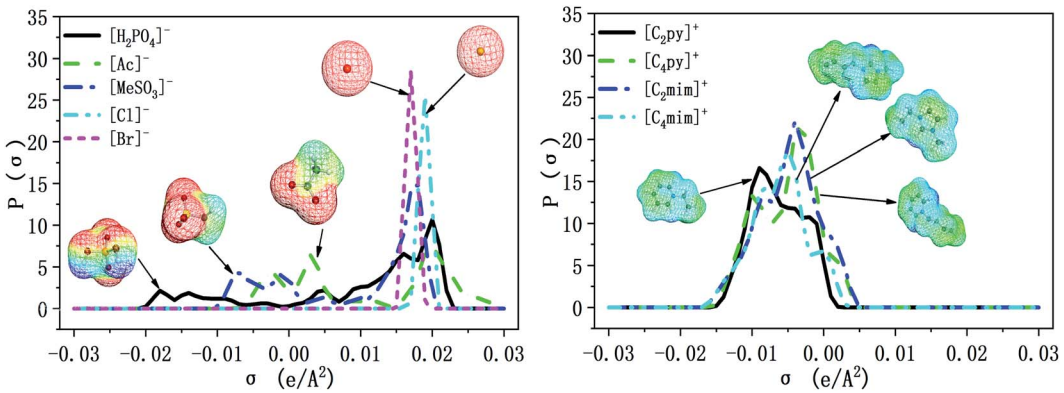

Fig. 5 σ-Surface and σ-profile of studied anions and cations.

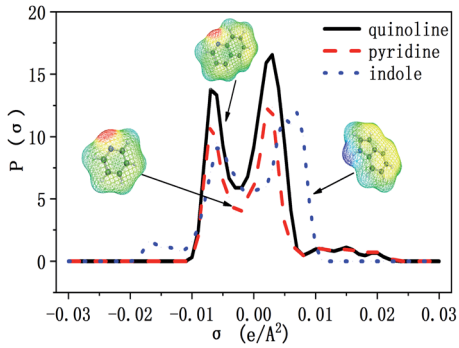

Fig. 6 σ-Surface and σ-profile of quinoline, pyridine and indole.

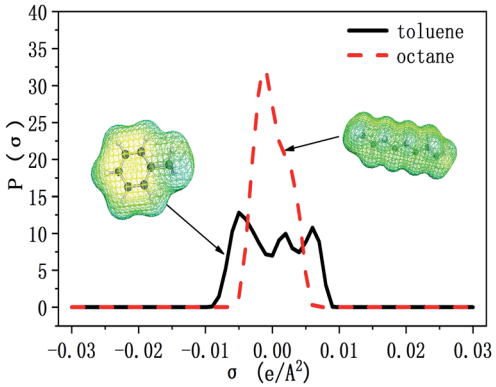

Fig. 7 σ-Surface and σ-profile of toluene and octane.

correspond to the red part in the σ-surface diagram and they can be used as HB receptors and have HB receptor energy. The peaks of indole are located in the polar region of $\sigma < -0.0082$ e Å^{-2}, which correspond to the blue part in Fig. 6 indicating that indole can be used as HB donor and has high HB donor energy. Therefore, strong hydrogen bond can be formed between the studied anions and indole, making the ILs highly selective to indole than to pyridine and quinoline.

The selectivity of ILs to indole in octane is still higher than that in toluene. As shown in Fig. 9, ILs composed of $[Ac]^-$, showed higher selectivity to indole. This can be explained with the aid of σ theory.[23,27] As depicted in Fig. 5, $[Ac]^-$, $[MeSO_3]^-$ and $[H_2PO_4]^-$ show the π electron cloud density, which correspond to the yellow part. However, the yellow area of $[Ac]^-$ is the largest, revealing that the π electron cloud density of $[Ac]^-$ is the highest. As discussed above, the π electron cloud density of indole is also the higher than pyridine and quinoline. This can lead to a strong π–π interaction between $[Ac]^-$ and indole, which further lead to higher selectivity to indole. This is consistent with the observations reported by of Hizaddin *et al.*,[59] and they found that the electronegativity of $[Ac]^-$ is strong, which can easily form hydrogen bond with indole molecules. Therefore, $[Ac]^-$ based ILs have higher selectivity to indole.

In a summary, $[Ac]^-$ (as HB receptor) have hydrogen bonding and π–π interaction with indole (as HB donor), results in higher selectivity of ILs to indole. From Fig. 9, $[C_2py][Ac]$ and $[C_2mim][Ac]$ are finally selected to remove the non-basic N-compounds in shale oil.

3.2.4. Mechanism of EDN by ILs. In a word, IL, as extracting agent in EDN, can extract N-compounds from oil-phase to IL-phase because ILs have big selectivity for N-components. This is mainly ascribed to the hydrogen bond and π–π interaction formed between the anions of ILs and the N-compounds in shale oil.

3.3 Solubility of ILs in shale oil

In addition to the selectivity of ILs for N-components, the solubility of ILs with shale oil also has great importance in the denitrification process since this can lead to the loss of ILs and the contamination of shale oil. The solubility of ILs, *i.e.*, $[C_4py][H_2PO_4]$, $[C_4mim][H_2PO_4]$, $[C_4py][MeSO_3]$, $[C_4mim][MeSO_3]$, $[C_2py][Ac]$ and $[C_2mim][Ac]$, with shale oil is computed by COSMO-RS which is shown in Fig. 10. According to Fig. 10, the solubility of ILs in shale oil is low in whole, ranging from 10^{-7} (ref. 38) to 10^{-3} (ref. 43). It is also observed that the solubility of ILs follows the trend: $[C_4py][H_2PO_4] < [C_4mim][H_2PO_4] <$

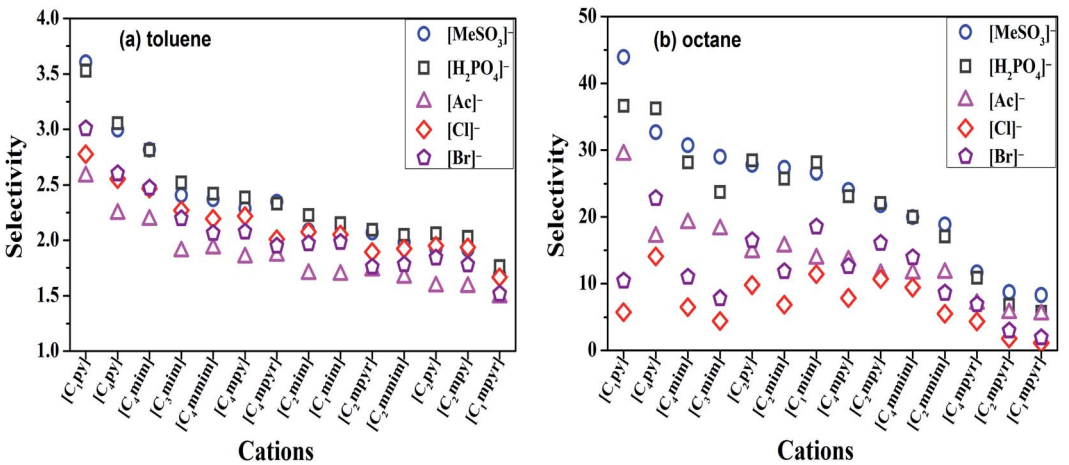

Fig. 8 Selectivity of ILs for quinoline in (a) toluene and (b) octane.

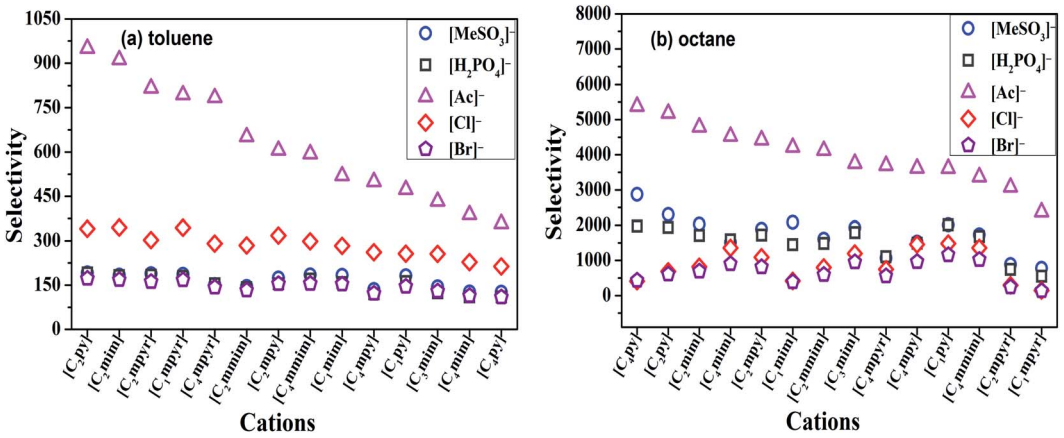

Fig. 9 Selectivity of ILs for indole in (a) toluene and (b) octane.

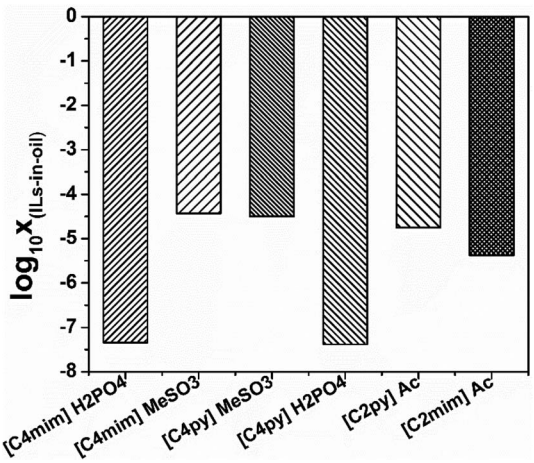

Fig. 10 Solubility of ILs with shale oil.

$[C_2mim][Ac] < [C_2py][Ac] < [C_4py][MeSO_3] < [C_4mim][MeSO_3]$. These results reveal that the solubility strongly depends on the structure of anions, also, the stronger is the polarity of anions, less is the solubility of ILs, as depicted in Fig. 5 and 10. Therefore, $[C_4py][H_2PO_4]$, $[C_4mim][H_2PO_4]$, $[C_2mim][Ac]$ and $[C_2py][Ac]$, exhibiting larger selectivity for N-components and smaller solubility with shale oil, are finally selected as suitable candidate solvents in denitrification of shale oil.

3.4 Extractive denitrification of shale oil

3.4.1. Extractive denitrification by ILs. As shown in Fig. 11, the EDN efficiency of shale oil by ILs, *i.e.*, $[C_4py][H_2PO_4]$, $[C_4mim][H_2PO_4]$, $[C_2mim][Ac]$ and $[C_2py][Ac]$, are investigated. The results show that $[C_4py][H_2PO_4]$ and $[C_4mim][H_2PO_4]$ exhibited the highest EDN efficiency of 100% for quinoline and pyridine; while $[C_2mim][Ac]$ and $[C_2py][Ac]$ have the highest EDN efficiency about 91% for indole, which indicates that ILs selected from COSMO-RS prediction have good denitrification performance. The regeneration and recycling of ILs are very important in their industrial applications. In this work, we chose $[C_4mim][H_2PO_4]$ as a representative to study its reusability in EDN process and the results are shown in Fig. 12. It is indicated that, after regeneration of four cycles, $[C_4mim][H_2PO_4]$ behaves similarly as fresh ILs, with a minute loss of N-removal efficiency of only <5% at the same experimental conditions. Therefore, the IL has proven to serve as a good extractant as well as a suitable candidate for the industrial application.

3.4.2. Revisit experimental results to COSMO-RS prediction. The experimentally determined EDN efficiency of shale oil is shown in Fig. 11. The removal efficiency for pyridine, quinoline and indole by different ILs follows $[C_4py][H_2PO_4] = [C_4mim][H_2PO_4] > [C_2mim][Ac] > [C_2py][Ac]$, $[C_4py][H_2PO_4] = [C_4mim][H_2PO_4] > [C_2py][Ac] > [C_2mim][Ac]$, $[C_2mim][Ac] > [C_2py][Ac] > [C_4mim][H_2PO_4] > [C_4py][H_2PO_4]$, respectively. These results are in agreement with the COSMO-RS prediction that ILs composed of $[H_2PO_4]^-$ showed higher selectivity to the basic N-compounds quinoline and pyridine, while ILs composed of $[Ac]^-$ showed higher selectivity to the non-basic N-compounds indole.

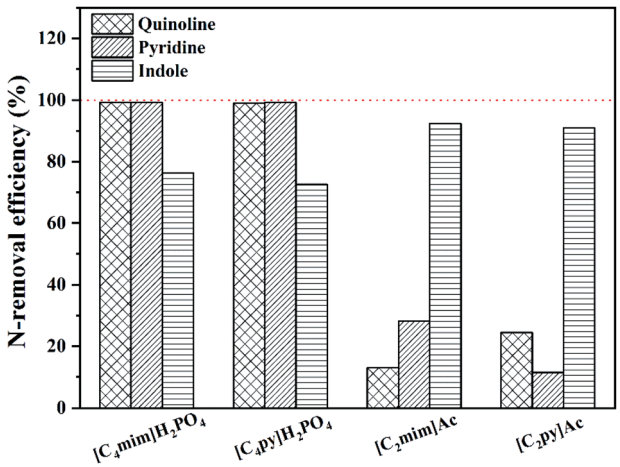

Fig. 11 N-removal efficiency of different ILs for different N-compounds in model shale oil (time 1 h, mass ration of IL/oil 1 : 2, temperature 40 °C).

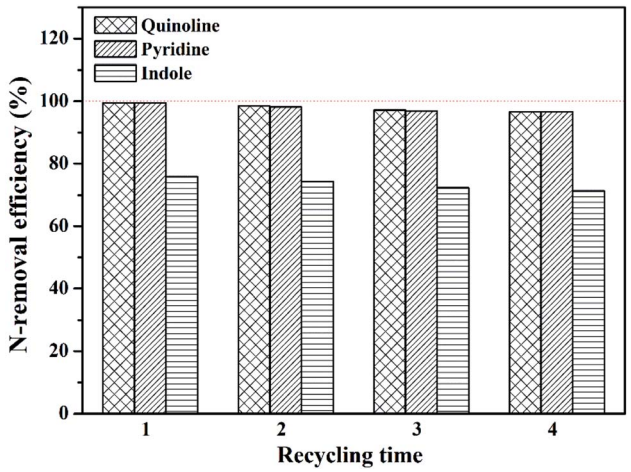

Fig. 12 The N-extraction efficiency *vs.* recycling time in extracting nitrides from shale oil by $[C_4mim][H_2PO_4]$ (extraction time 1 h, mass ration of IL/oil 1 : 2, temperature 40 °C).

4. Conclusion

In present work, the selectivity of 70 ILs to pyridine, quinoline and indole was determined employing COSMO-RS. The influence of ILs structural characteristics, composition of shale oil and properties of N-compounds are investigated from micro-level view with σ-surface and σ-profile. On the basis of the selectivity, we selected 6 ILs and studied their solubility with shale oil. Finally, we selected ILs exhibiting higher selectivity to N-components and lower solubility with shale oil, as suitable candidate solvents in the EDN experiment. The present study has drawn the conclusions as: (1) the selectivity has strong dependence on anion species, and it is greatly influenced by hydrogen bonding (HB) and π–π interaction between ILs and N-compounds. (2) ILs composed $[H_2PO_4]^-$ and $[MeSO_3]^-$ with higher HB donor energy showed higher selectivity to the basic N-compounds quinoline and pyridine; ILs composed of $[Ac]^-$ with larger π electron cloud density, showed higher selectivity to the non-basic N-compounds indole. (3) ILs composed of anions that with stronger polarity, exhibited less solubility with shale oil. (4) The four selected ILs ($[C_4py][H_2PO_4]$, $[C_4mim][H_2PO_4]$, $[C_4py][MeSO_3]$ and $[C_4mim][MeSO_3]$) are investigated experimentally. The COSMO-RS prediction are obtained in good agreement with experimental results. This work presents a theoretical basis to design and select the desirable ILs with higher selectivity to N-compounds and smaller solubility with shale oil for use in denitrification of shale oil.

Conflicts of interest

There are no conflicts to declare.

Acknowledgements

The authors wish to acknowledge the financial support by the National Natural Science Foundation of China (No. 52006068) and the Fundamental Research Funds for the Central Universities (No. 2020MS060).

References

1 H. Yu, S. Li and G. Jin, Hydrodesulfurization and hydrodenitrification of diesel distillate from Fushun shale oil, *Oil Shale*, 2010, **27**, 126–134.
2 P. T. Williams and H. M. Chishti, Reaction of nitrogen and sulphur compounds during catalytic hydrotreatment of shale oil, *Fuel*, 2001, **80**, 957–963.
3 H. M. Chishti and P. T. Williams, Aromatic and hetero–aromatic compositional changes during catalytic hydrotreatment of shale oil, *Fuel*, 1999, **78**, 1805–1815.
4 S. R. Gao, S. F. Fang, R. Z. Song, X. C. Chen and G. R. Yu, Extractive Denitrogenation of Shale Oil Using Imidazolium Ionic Liquids, *Green Energy Environ.*, 2020, **5**, 173–182.
5 L. C. Gutberlet and R. J. Bertolacini, Inhibition of hydrodesulfurization by nitrogen compounds, *Ind. Eng. Chem. Process Des. Dev.*, 1983, **22**, 246–250.
6 M. J. Girgis and B. C. Gates, Reactivities, reaction networks, and kinetics in high–pressure catalytic hydroprocessing, *Ind. Eng. Chem. Res.*, 1991, **30**, 2021–2058.
7 J. R. Katzer and R. Sivasubramanian, Process and Catalyst Needs for Hydrodenitrification, *Catal. Rev.: Sci. Eng.*, 1979, **20**, 155–208.
8 M. A. Greaney, J. N. Begasse and M. Lee, Acid extraction for denitrification of middle distillates and lube oil fractions using spent sulfuric acid from alkylation processes, WO Patent No. 2005056726, 2005.
9 M. Macaud, M. Sevignon, A. Favre-Reguillon, M. Lemaire, E. Schulz and M. Vrinat, Novel Methodology toward Deep Desulfurization of Diesel Feed Based on the Selective Elimination of Nitrogen Compounds, *Ind. Eng. Chem. Res.*, 2004, **43**, 7843–7849.
10 T. Koltai, M. Macaud, A. Guevara, E. Schulz, M. Lemaire, R. Bacaud and M. Vrinat, Comparative inhibiting effect of polycondensed aromatics and nitrogen compounds on the hydrodesulfurization of alkyldibenzothiophenes, *Appl. Catal., A*, 2002, **231**, 253–261.
11 S. R. Gao, X. C. Chen, R. Abro, A. A. Abdeltawab, S. S. Al-Deyab and G. R. Yu, Desulfurization of fuel oils: mutual solubility of ionic liquids and fuel oil, *Fuel*, 2016, **173**, 164–171.
12 S. R. Gao, X. C. Chen, R. Abro, A. A. Abdeltawab, S. S. Al-Deyab and G. R. Yu, Desulfurization of fuel oil: conductor-like screening model for real solvents study on capacity of ionic liquids for thiophene and dibenzothiophene, *Ind. Eng. Chem. Res.*, 2015, **54**, 9421–9430.
13 S. R. Gao, X. C. Chen, R. Abro, A. A. Abdeltawab, S. S. Al-Deyab and G. R. Yu, Mutual Solubility of Acidic Ionic Liquid and Model Gasoline of n-Octane + 1–Octene + Toluene, *J. Taiwan Inst. Chem. Eng.*, 2016, **69**, 78–84.
14 S. R. Gao, J. J. Li, A. A. Abdeltawab, S. S. Al-Deyab and G. R. Yu, A combination desulfurization method for diesel fuel: oxidation by ionic liquid with extraction by solvent, *Fuel*, 2018, **224**, 545–551.

15 S. R. Gao, X. C. Chen, X. T. Xi, M. Abro and G. R. Yu, Coupled Oxidation–Extraction Desulfurization: A Novel Evaluation for Diesel Fuel, *ACS Sustainable Chem. Eng.*, 2019, **7**, 5660–5668.

16 H. Zhao, H. Gao, G. Yu, Q. Li and Z. Lei, Capturing methanol and dimethoxymethane gases with ionic liquids, *Fuel*, 2019, **241**, 704–714.

17 G. Yu, Y. Jiang, J. Cheng and Z. Lei, Structural effect on the vapor–liquid equilibrium of toluene–ionic liquid systems, *Chem. Eng. Sci.*, 2019, **198**, 1–15.

18 Z. Lei, C. Dai, X. Liu, L. Xiao and B. Chen, Extension of the UNIFAC model for ionic liquids, *Ind. Eng. Chem. Res.*, 2012, **51**, 12135–12144.

19 J. Han, C. Dai, Z. Lei and B. H. Chen, Gas drying with ionic liquids, *AIChE J.*, 2018a, **64**, 606–619.

20 C. Dai, Z. Lei and B. Chen, Gas solubility in long-chain imidazoliumbased ionic liquids, *AIChE J.*, 2017, **63**, 1792–1798.

21 J. Eber, P. Wasserscheid and A. Jess, Deep desulfurization of oil refinery streams byextraction with ionic liquid, *Green Chem.*, 2004, **6**, 314–322.

22 L. L. Xie, A. Favre-Reguillon, S. Pellet-Rostaing, X. X. Wang, X. Fu, J. Estager, M. Vrinat and M. Lemaire, Selective Extraction and Identification of Neutral Nitrogen Compounds Contained in Straight–Run Diesel Feed Using Chloride Based Ionic Liquid, *Ind. Eng. Chem. Res.*, 2008, **47**, 8801–8807.

23 S. Zhang, Q. Zhang and Z. C. Zhang, Extractive desulfurization and denitrification of fuels using ionic liquids, *Ind. Eng. Chem. Res.*, 2004, **43**, 614–622.

24 J. Eßer, P. Wasserscheid and A. Jess, Deep desulfurization of oil refinery streams by extraction with ionic liquids, *Green Chem.*, 2004, **6**, 316–322.

25 C. Asumana, G. R. Yu, Y. W. Guan, S. D. Yang, S. Z. Zhou and X. C. Chen, Extractive denitrification of fuel oils with dicyanamide-based ionic liquids, *Green Chem.*, 2011, **13**, 3300–3305.

26 Y. Zhang, D. W. Shang and X. Li, *Proceedings of the First BUCT Innovative Entrepreneurship Forum*, 2012.

27 X. C. Chen, S. Yuan, A. A. Abdeltawab, S. S. Al-Deyab, J. W. Zhang, L. Yu and G. R. Yu, Extractive desulfurization and denitrification of fuels using functional acidic ionic liquids, *Sep. Purif. Technol.*, 2014, **133**, 187–193.

28 H. Wang, C. Xie and S. Yu, Denitrification of simulated oil by extraction with H_2PO_4-based ionic liquids, *Chem. Eng. J.*, 2014, **237**, 286–290.

29 M. R. Shah and G. D. Yadav, Prediction of liquid−liquid equilibria of (aromatic+aliphatic+ionic liquid) systems using the Cosmo-SAC model, *J. Chem. Thermodyn.*, 2012, **49**, 62–69.

30 R. Sadeghi, A modified Wilson model for the calculation of vapour + liquid equilibrium of aqueous polymer+ salt solutions, *J. Chem. Thermodyn.*, 2005, **37**, 323–329.

31 R. S. Santiago, G. R. Santos and M. Aznar, UNIQUAC correlation of liquid–liquid equilibrium in systems involving ionic liquids: the DFT–PCM approach. Part II, *Fluid Phase Equilib.*, 2010, **293**, 66–72.

32 H. F. Hizaddin, M. K. Hadj-Kali and A. Ramalingam, Extraction of nitrogen compounds from diesel fuel using imidazolium and pyridinium based ionic liquids: experiments, COSMO–RS prediction and NRTL correlation, *Fluid Phase Equilib.*, 2015, **405**, 55–67.

33 U. Domanska, M. Królikowski, D. Ramjugernath, T. M. Letcher and K. Tumba, Phase equilibria and modeling of pyridinium-based ionic liquid solutions, *J. Phys. Chem. B*, 2010, **114**, 15011–15017.

34 M. G. Freire, L. M. N. B. F. Santos, I. M. Marrucho and J. A. P. Coutinho, Evaluation of COSMO-RS for the prediction of LLE and VLE of alcohols + ionic liquids, *Fluid Phase Equilib.*, 2007, **255**, 167–178.

35 B. Schröder and J. A. Coutinho, Predicting enthalpies of vaporization of aprotic ionic liquids with COSMO-RS, *Fluid Phase Equilib.*, 2014, **370**, 24–33.

36 T. Su, Z. Tang, C. Yin, Y. Yang, H. Wang, L. Peng, Y. Su, P. Su and J. Li, Insights into quaternary ammonium-based ionic liquids series with tetrafluoroborate anion for CO_2 capture, *J. Mol. Liq.*, 2020, 114857.

37 Z. Song, T. Zhou, Z. Qi and K. Sundmacher, Systematic Method for Screening Ionic Liquids as Extraction Solvents Exemplified by an Extractive Desulfurization Process, *ACS Sustainable Chem. Eng.*, 2017, **5**, 3382–3389.

38 S. Dezhang, F. Huisheng, X. Feng, L. Wenxiu and Z. Zhigang, Evaluation of COSMO-RS model for the LLE prediction of benzene plus cyclohexane plus ionic liquid system, *J. Chem. Thermodyn.*, 2020, **145**, 106032.

39 Z. Rashid, C. D. Wilfred, N. Gnanasundaram, A. Arunagiri and T. Murugesan, Screening of ionic liquids as green oilfield solvents for the potential removal of asphaltene from simulated oil: COSMO-RS model approach, *J. Mol. Liq.*, 2018, **255**, 492–503.

40 J. L. Han, C. N. Dai, G. Q. Yu and Z. G. Lei, Parameterization of COSMO-RS model for ionic liquids, *Green Energy Environ.*, 2018, **3**, 247–265.

41 J. Fang, R. Zhao, W. Su, C. Li, J. Liu and B. Li, A molecular design method based on the COSMO-SAC model for solvent selection in ionic liquid extractive distillation, *AIChE J.*, 2016, **62**, 2853–2869.

42 H. Grensemann and J. Gmehling, Performance of a Conductor-Like Screening Model for Real Solvents Model in Comparison to Classical Group Contribution Methods, *Ind. Eng. Chem. Res.*, 2005, **44**, 1610–1624.

43 H. W. Khan, A. V. B. Reddy, M. M. E. Nasef, M. A. Bustam and M. Moniruzzaman, Screening of ionic liquids for the extraction of biologically active compounds using emulsion liquid membrane: COSMO-RS prediction and experiments, *J. Mol. Liq.*, 2020, **309**, 113122.

44 T. Banerjee, K. K. Verma and A. Khanna, Liquid–liquid equilibrium for ionic liquid systems using COSMO-RS: effect of cation and anion dissociation, *AIChE J.*, 2008, **54**, 1874–1885.

45 J. P. Gutiérrez, G. W. Meindersma and A. B. de Haan, COSMO-RS-Based Ionic-Liquid Selection for Extractive Distillation Processes, *Ind. Eng. Chem. Res.*, 2012, **51**, 11518–11529.

46 Y. Zhou, D. Xu, L. Zhang, Y. Ma, X. Ma, J. Gao and Y. Wang, Separation of thioglycolic acid from its aqueous solution by ionic liquids: ionic liquids selection by the COSMO-SAC model and liquid-liquid phase equilibrium, *J. Chem. Thermodyn.*, 2018, **118**, 263–273.

47 A. A. P. Kumar and T. Banerjee, Thiophene separation with ionic liquids for desulphurization: a quantum chemical approach, *Fluid Phase Equilib.*, 2009, **278**, 1–8.

48 R. Anantharaj and T. Banerjee, COSMO-RS based predictions for the desulphurization of diesel oil using ionic liquids: effect of cation and anion combination, *Fuel Process. Technol.*, 2011, **92**, 39–52.

49 Z. Song, X. Hu, Y. Zhou, T. Zhou, Z. Qi and K. Sundmacher, Rational design of double salt ionic liquids as extraction solvents: separation of thiophene/n-octane as example, *AIChE J.*, 2019, **65**, 16625.

50 S. M. Vilas-Boas, G. Teixeira, S. Rosini, M. A. R. Martins, P. S. Gaschi, J. A. P. Coutinho, O. Ferreira and S. P. Pinho, Ionic liquids as entrainers for terpenes fractionation and other relevant separation problems, *J. Mol. Liq.*, 2020, 114647.

51 A. R. Ferreira, M. G. Freire, J. C. Ribeiro, F. M. Lopes, J. G. Crespo and J. A. Coutinho, Overview of the liquid–liquid equilibria of ternary systems composed of ionic liquid and aromatic and aliphatic hydrocarbons, and their modeling by COSMORS, *Ind. Eng. Chem. Res.*, 2012, **51**, 3483–3507.

52 A. Klamt and F. Eckert, COSMO-RS: a novel and efficient method for the a priori prediction of thermophysical data of liquids, *Fluid Phase Equilib.*, 2000, **172**, 43–72.

53 A. Klamt, F. Eckert and W. Arlt, COSMO-RS: an alternative to simulation for calculating thermodynamic properties of liquid mixtures, *Annu. Rev. Chem. Biomol. Eng.*, 2010, **1**, 101–122.

54 A. R. Ferreira, M. G. Freire, J. C. Ribeiro, F. M. Lopes, J. G. Crespo and J. A. P. Coutinho, Ionic liquids for thiols desulfurization: experimental liquid–liquid equilibrium and COSMO–RS description, *Fuel*, 2014, **128**, 314–329.

55 Z. G. Lei, B. H. Chen and C. Y. Li, COSMO–RS modeling on the extraction of stimulant drugs from urine sample by the double actions of supercritical carbon dioxide and ionic liquid, *Chem. Eng. Sci.*, 2007, **62**, 3940–3950.

56 A. R. Ferreira, M. G. Freire, J. C. Ribeiro, F. M. Lopes, J. G. Crespo and J. A. P. Coutinho, An overview of the liquid–liquid equilibria of (ionic liquid+hydrocarbon) binary systems and their modeling by the Conductor–Like Screening Model for Real Solvents, *Ind. Eng. Chem. Res.*, 2011, **50**, 5279–5294.

57 A. Klamt, *COSMO-RS: from quantum chemistry to fluid phase thermodynamics and drug design*, Elsevier, 2005.

58 I. Anugwom, P. Mäki-Arvela, T. Salmi and J. P. Mikkola, Ionic liquid assisted extraction of nitrogen and sulphur–containing air pollutants from model oil and regeneration of the spent ionic liquid, *J. Environ. Protect.*, 2011, **2**, 796–802.

59 H. F. Hizaddin, M. A. Hashim and R. Anantharaj, Evaluation of Molecular Interaction in Binary Mixture of Ionic Liquids+Heterocyclic Nitrogen Compounds: Ab Initio Method and COSMO–RS Model, *Ind. Eng. Chem. Res.*, 2013, **52**, 18043–18058.